

# How long do we stand our colleagues? A universal behavior in face-to-face relations

Stéphane Plaszczynski\* and Gilberto Nakamura  
*Université Paris-Saclay, CNRS/IN2P3, IJCLab, 91405 Orsay, France and  
 Center for Interdisciplinary Research in Biology (CIRB),  
 Collège de France, CNRS, INSERM, Université PSL, Paris, France.*  
 (Dated: February 14, 2023)

**Abstract** We compare face-to-face interaction data recorded by wearable sensors in various sociological environments. The interactions among individuals display a clear environment-dependent diversity in agreement with previous analyses. The contact durations follow heavy-tailed distributions although not exactly of power-law type as previously suggested. Guided by the common patterns observed for each relation, we introduce a variable named the duration contrast, which reveals a common behavior among all datasets. This suggests that our tendency to spend more or less time than usual with a given individual in a face-to-face relation is not governed by social rules but by a common human trait. Additional data shows that it is the same for baboons. Furthermore, we propose a new kind of model to describe the contacts in a given relation based on the recently introduced concept of Levy Geometric Graphs. It reproduces the data at an impressive level. The associated Levy index is found to be  $\alpha = 1.1$  on all the datasets, suggesting a universal law for primates and opening many exciting perspectives.

**Significance statement** By comparing face-to-face interaction data obtained in very different environments (a hospital in France, an international conference in Italy, a small village in Africa) we show that the deviation from the average duration of contact between each pair of individuals (the duration contrast) follows in each case a very similar statistical law. Surprisingly, the same distribution is observed among a population of baboons. It suggests that our tendency to deviate from the usual (mean) time spent in any face-to-face relation is primarily independent of the sociological environment and governed by its own rules. To explicit them, we propose an original model based on a random Levy-walk in a 2D space of relation, that perfectly reproduces the data.

## INTRODUCTION

Since the advent of the Internet at the dawn of the XXth century, the quantity of digital data describing our behavior has inflated, offering to scientists an unprecedented opportunity to study human interactions in a more quantitative way. This opened the field of sociology to data-analysis and from the hard-science community, came the tacit idea that complex human behaviors can be modeled as simple systems [1–6]. With the rapid development of mobile technologies (GPS, Bluetooth, cellphones) a lot of effort was first put in trying to capture the patterns of human mobility (for a review, see [7]). A more local picture of our everyday social interactions can be obtained using dedicated proximity sensors. Following a pioneering experiment that equipped conference participants with pocket switched devices [8, 9], the *sociopatterns* collaboration ([www.sociopatterns.org](http://www.sociopatterns.org)) developed wearable sensors that allow to register the complex patterns of face-to-face interactions [10, 11]. The radio-frequency signal is only

recorded if two individual are in front of each other for a duration of a least 20 s (which is the timing resolution). We note that, from a sociological point of view, a distance below 1.5 m covers the traditional *private* (< 50 cm), *personal* (< 1.2 m) and *social* (< 3.5 m) zones. The goal is not only to analyze social interactions but also to understand how information (or even a disease) spreads over a real dynamical network [12–15]. Those sensors were worn by volunteers in several work-related environments: scientific conferences [10, 12, 13], a hospital ward [16], an office [15] and at school [17, 18]. As part of a UNICEF program, they were also used to characterize social exchanges in small villages in Kenya and Malawi [19, 20] and for ethological studies on baboons [21]. It was rapidly noticed (see [22] for a short review) that the duration of face-to-face contacts follows a broad distribution, sometimes qualified a bit rapidly as a “power-law”, and that it was similar among participants in several environments.

We wish to revisit here in detail this assertion. Most importantly, the comparisons performed so far applied to some very similar sociological environments (conferences, high-school, office...) which are typically occidental (french), educated and with a scientific background. It is unclear to which level they are general. We thus also compare those data to the ones from rural Malawi, and baboon interactions.

After describing our data selection and some methodological difference with previous studies in Sect. I, we will show in Sect. II, that social interactions between individuals are very different in each environment. We will then study the temporal aspects of each relation in Sect. III introducing the concept of contrast for contact duration. It will be shown that its distribution is essentially the same for each dataset and for each relation individually. We then present in Sect. IV a model completely different from previously proposed ones. Indeed, it is not agent-based but describes the relation itself. Based on a recent theoretical work on Levy Geometric Graphs [23], we will show that it reproduces perfectly the data. This model raises questions that will be discussed in Sect. V. Some extra information, referred to in the text, is given in the *Supporting*

\* [stephane.plaszczynski@ijclab.in2p3.fr](mailto:stephane.plaszczynski@ijclab.in2p3.fr)

Information (SI) document.

## I. MATERIAL AND METHODS

### A. Datasets

We have chosen 4 datasets sociologically most dissimilar.

1. *hosp*: these are early data collected over 3 days [24] on 75 participants in the geriatric unit of a hospital in Lyon (France) [16]. Most interactions (75%) involve nurses and patients (not doctors) so we consider that sample to be sociologically quite different from the next (scientific) one.
2. *conf*: these are also some early classical data from the ACM Hypertext 2009 conference ([www.ht2009.org](http://www.ht2009.org)) that involved about a hundred of participants for 3 days [13] in Torino (Italy). The audience is international with a scientific background. There exist also some data taken at another conference in Nice in 2009 (SFHH, [25]) with more participants, but we prefer to use the former which has a number of individuals comparable to the other datasets. However we have checked that we obtain similar results with the SFHH data.
3. *malawi*: those proximity data were taken in a small village of the district of Dowa in Malawi (Africa) where 86 participants agreed to participate for 13 (complete) days. Interestingly those data contain both extra and intra-household interactions, although we will not split them in the following. This community consists essentially of farmers.
4. *baboons* Those data were taken at a CNRS Primate Center near Marseille (France) where 13 baboons were equipped with the sensors for a duration of 26 days. The goal was to study their interactions, and study how conclusions reached from data-analysis match those provided by standard observation.

With that choice, we span very different sociological environments. We have also analyzed a few other datasets collected at the SFHH conference, an office and a high-school. They give similar results but we consider them as sociologically closer to the *conf* one. A valuable interest, is that those data were taken with the very same devices, and can be compared immediately, minimizing possible sources of systematic errors.

### B. Differences with previous studies

Previous studies considered the overall temporal properties of interactions, i.e. without differentiating the pair of people interacting. In this work we will put accent on the temporal properties of each pair separately.

Probability distribution functions (p.d.f) are often estimated by histograms, i.e. by counting the number of samples that

falls within some bins. But for heavy-tailed distributions the size of the bins is delicate to choose. With a constant size binning, several bins end up empty for large values. Using a logarithmically increasing binning is neither a solution since it supposes that the distribution is constant on the wide range of last bins. Following [26], we will use instead the *probability to exceed* function (p.t.e, also known as the “complementary cumulative distribution function”, CCDF) which is computed simply by sorting the samples and plotting them with respect to their relative frequency. In this way, one does not need to define a binning. If the p.d.f follows a power-law its p.t.e also. Conversely, if the p.t.e plotted on logarithmic axes is not linear, its p.d.f is not a power-law neither.

## II. SOCIAL INTERACTIONS BETWEEN INDIVIDUALS

The structure of social interactions between individuals can be studied through time-aggregated graphs representing any ( $> 20$  s) face-to-face interaction in a given time window. Since those interactions most often repeat on a day-by-day basis, we give results on a complete day (24 h). The graphs obtained for the first day are shown on Figure 1, and we checked that they are similar for the others.

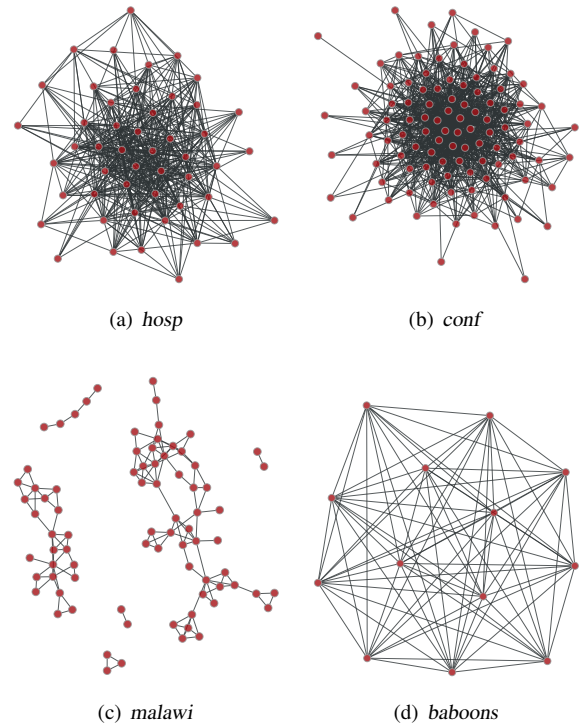


Figure 1. Aggregated graphs of interactions over one day for our 4 datasets. Vertices (red points) represent agents and there is a link (edge) if a face-to-face interaction occurred for more than 20 s.

The graphs for the *hosp* and especially the *conf* datasets show a strongly connected core. The *malawi* one is much sparser, while the *baboons* one is almost complete showing that each animal interact with all the others.

Table I. Properties of time aggregated graphs on each dataset per day. Uncertainties are the standard deviations between the days.  $T$  is the number of (complete) days in the dataset.  $N$  the number of interacting agents.  $\langle k \rangle$  is the mean degree, i.e. the average number of agents each individual interacts with during one day.  $\langle w \rangle$  is the mean weight where the weights specify the total duration of a single relation [27]. Mean strength  $\langle s \rangle$  which represents the average total interaction time per individual.

group	T	N	$\langle k \rangle$	$\langle w \rangle$ (mins)	$\langle s \rangle$ (mins)
<i>hosp</i>	3	$49 \pm 1$	$18 \pm 1$	$6 \pm 13$	$97 \pm 101$
<i>conf</i>	3	$100 \pm 3$	$20 \pm 1$	$2 \pm 14$	$46 \pm 63$
<i>malawi</i>	12	$70 \pm 4$	$3 \pm 1$	$24 \pm 37$	$65 \pm 74$
<i>baboons</i>	26	$13 \pm 1$	$11 \pm 1$	$8 \pm 11$	$87 \pm 53$

Table I gives a more quantitative view of some of the graph's properties. The number of different people met per day (the degree of the graphs) is about 20 in both the hospital and the conference environments. As is apparent in Figure 1(c), it is much smaller in the rural community (3). But the interaction times are longer ( $\approx 25$  min) which reflect different sector of activities (agrarian and including inter-housing relations for the *malawi* data).

The strength of the relation represents the total time per individual spent interacting with others per day. It is essentially the product of the mean number of people met per day and the time spent interacting with them ( $\langle s \rangle \approx \langle k \rangle \langle w \rangle$ ). It varies by a factor of two (from 45 min to 1.5 h) although the large standard-deviations indicates important daily variations due to the heavy-tail of the distribution.

The comparison to the *baboons* dataset should be handled with care since there is a much smaller number of agents (13). Since the baboons interact essentially all with each other (Figure 1(d)), their mean degree is bounded,  $\langle k \rangle \approx N$ . On the other hand, their small number probably increases their interaction duration ( $\langle w \rangle$ ) so that the strength of their relation is finally similar to that of the human groups.

The goal of this short section is not to enter into the detail of the differences but to highlight that, as expected, those heterogeneous sociological groups have some very different interaction patterns between individuals.

### III. FACE-TO-FACE TEMPORAL RELATION

We consider now the duration of all interactions between individuals. Figure 2 shows the distribution for each group. They are indeed “heavy-tailed”; most interactions are short time (at the minute level) but some may drift up to an hour. Although it is often claimed that these distributions follow a “power-law” (which would look linear in the logarithmic representation) this more precise approach, using the p.t.e, shows that it is only true over a limited range or rather that a curvature exists. Interactions for people in *malawi* tend to last longer than for all the others. The baboons’ duration of interaction is similar to the human ones (as noticed in [21]), although there are some sizable differences at short times, somewhat squeezed by the logarithmic scale. Overall, at the level

of precision we wish to investigate, we consider these distributions as quite different and not following a power-law.

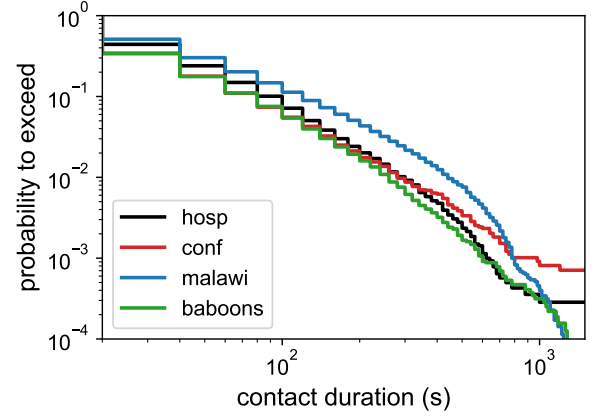


Figure 2. Distribution (p.t.e) of the contact duration on the four datasets (all days used).

We focus on the detail of each relation, i.e. pair of individuals, corresponding to edges in time-aggregated graphs. Each one consists in a set of intervals measuring the beginning and end times of each interaction at the resolution of the instruments (20 s). There is a varying number of interactions (intervals) per relation, that we call  $N_{int}(r)$ . In the following we will only consider the duration of the interactions (postponing inter-contact durations to the Discussion) that we note  $\{t_i(r)\}$ . They are variable-size timelines. Unless otherwise specified, they are expressed as a number of resolution steps.

The number of registered interactions for a given pair clearly depends on the total duration of the experiments (Table I) but we may compare it for one day, which then corresponds to a rate of interactions per day. The distribution of this variable is shown in Figure 3(a). It is clearly different for each group. People at the conference tend to interact (with the same person) less often. Frequently (65%) it is only once per day, against 25% for the *hosp* and *malawi* datasets, and 3% for *baboons*.

The mean interaction time per relation

$$\bar{t}(r) = \frac{1}{N_{int}(r)} \sum_{i=1}^{N_{int}(r)} t_i(r), \quad (1)$$

is shown in Figure 3(b). Here again distributions are heavy-tailed and different. There is a marked difference between animals and humans, the former interacting for shorter times.

We now introduce the contact duration contrast of a relation (or simply “contrast”) as the duration of each interaction scaled by its mean value

$$\delta_i(r) = \frac{t_i(r)}{\bar{t}(r)}. \quad (2)$$

It describes deviations with respect to the mean time of the relation and is a dimensionless quantity. We emphasize that the scaling by  $\bar{t}(r)$  is different for each pair of individuals (relation).

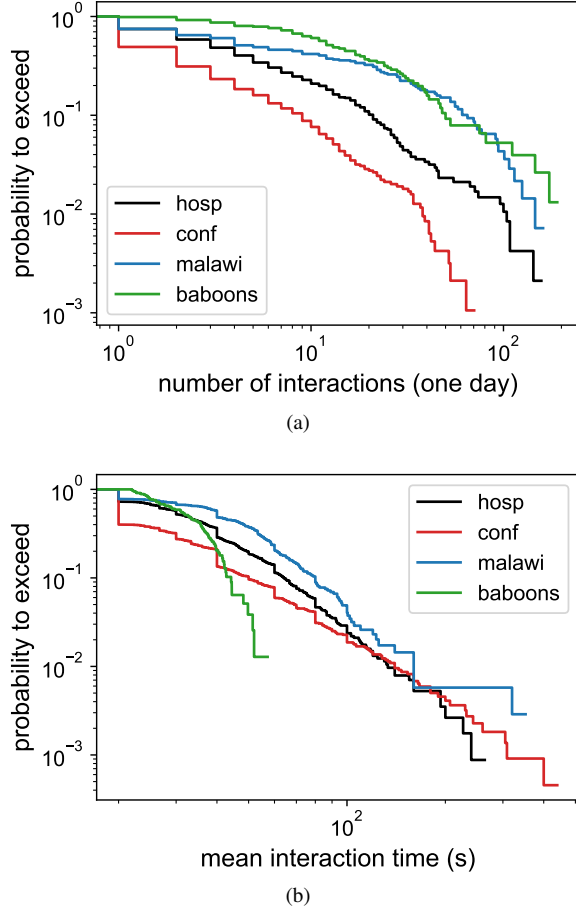


Figure 3. General characteristics of temporal relations on the 4 datasets. (a) Distribution (p.t.e) of the number of interactions per relation for one day, and (b) of the mean interaction time. To gain precision, we use the complete datasets for the latter.

When there are few samples, the arithmetic mean (eq. (1)) is a poor estimate of the true mean-time value. Furthermore, it is strongly correlated to the individual samples. The measured contrast is then very noisy. We thus apply a cut to select only timelines with a large number of samples. Since the time distributions are heavy-tailed, we require at least 50 samples to correctly estimate the mean ( $N_{int}(r) > 50$ ). Using the full datasets, we are left with respectively 57, 26, 91 and 70 timelines for the *hosp*, *conf*, *malawi* and *baboons* datasets. We show the p.t.e distributions of the contact duration contrast for the 4 groups in Figure 4.

They are strikingly similar up to a contrast of about 10. Small differences, barely noticeable in the linear representation Figure 4 (b), happen at low scales, but as we shall explain in Sect. IV, they are most probably due to the finite resolution of the instrument.

If we compare this distribution to Figure 2, we see that by dividing the duration by each individual mean-time, we have standardized the results. Strictly speaking, Figure 4 includes the  $N_{int} > 50$  cut on the number of interactions while Figure 2 does not, but a similar dispersion is observed on the latter

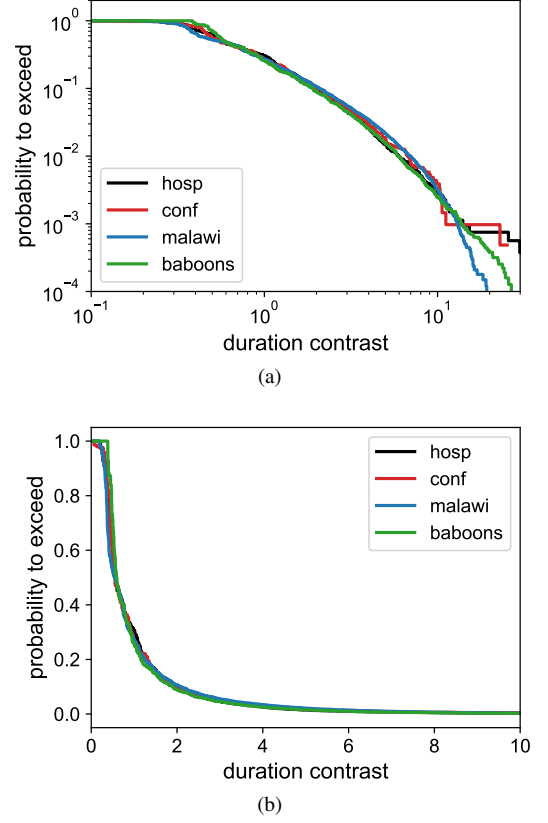


Figure 4. Distributions (p.t.e) of the duration contrast obtained for all relations within the same group satisfying  $N_{int}(r) > 50$  in logarithmic (a) and linear scales (b). Due to shorter data taking periods (see Table I), distributions for the *hosp* and *conf* datasets starts to become noisy for contrast above  $\approx 10$ .

when we include the cut (*SIAppendix, S1*). Similar results are obtained at another conference (SFHH), in an office and in a high-school (*SIAppendix, S2*).

One may think that this “universal” distribution is only valid for high-rate interactions since we have used the  $N_{int}(r) > 50$  cut. However this is only an experimental limitation; with a longer data-taking period most timelines would exceed 50 interactions and the mean time values would be known precisely. We argue that the universality is a more general feature and that the cut, used to clean the data, did not alter the underlying process but does only allow to reveal it. First we note that similar results are obtained with a lower cut value  $N_{int} > 30$  (*SIAppendix, S3*). We then show that we can still reproduce the contrast distribution without any cut, using only the distributions with the cut (Figure 4). To this purpose we perform Monte-Carlo simulations. For a given dataset, for each relation (without any cut), we draw  $N_{int}(r)$  random numbers following Figure 4 distribution to obtain  $\delta_{i=1, \dots, N_{int}}$  contrast values. Those samples are obtained from the distribution with the  $N_{int}(r) > 50$  cut, so with precise mean values that we call  $\mu$ . We may mimic the statistical fluctuations due to any



$N_{int}(r)$  value, by using the ratio

$$\delta_i^{mes} = \frac{\delta_i}{\frac{1}{N_{int}} \sum_i \delta_i} = \frac{t_i/\mu}{\frac{1}{N_{int}} \sum_i t_i/\mu} = \frac{t_i}{\bar{t}} \quad (3)$$

since  $\mu$  actually cancels out. We compare the measured contrast distribution to the one observed on data, this time without any  $N_{int}(r)$  cut, in Figure 5 for the *conf* dataset. We reproduce correctly the whole contrast distribution using only the Figure 4 one obtained with  $\approx 1\%$  of the data ( $N_{int} > 50$ ). Similar results are obtained for the other datasets (*SIAppendix, S4.1*). This shows that the contrast distributions obtained on the large sample statistics are sufficient to reproduce any number of interactions, including very low ones. In other words, the  $N_{int}(r) > 50$  cut only cleans the data without affecting the underlying “true” contrast distribution.

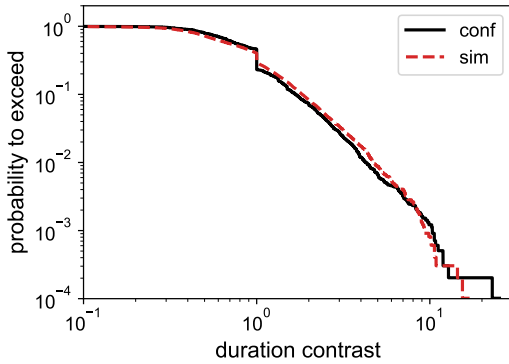


Figure 5. Distributions (p.t.e) of the duration contrast obtained for all relations in the *conf* dataset and simulations produced using the corresponding Figure 4 distribution (see text for details). The dip at 1 comes from numerous cases (65%) where  $N_{int}=1$  always leads to  $\delta = 1$ .

At this point we have shown that the *combined* contrast duration (i.e. for all relations) follows a very similar distribution. We now consider each relation separately and show in Figure 6 a superposition of the contrast duration distributions with the  $N_{int}(r) > 50$  cut (similar results are observed without it but are as expected more noisy, see *SIAppendix, S4.2*). They all follow rather closely the combined distribution, meaning that each relation is governed by the same universal rule. Without the cut, our simulations still reproduces correctly the spread observed for each relation (*SIAppendix, S4.2*).

We thus arrive at the astonishing conclusion, that our *individual* tendency to deviate from the mean time spent in a face-to-face relation with a given agent is essentially universal; it is the same in an occidental hospital ward or conference, and in a village in Malawi. It is also the same for social interactions among baboons in an enclosure.

#### IV. RELATION AS A LEVY PROCESS

We wish to model a relation as a random process, i.e the interaction between a *pair* of individuals by a *single* mechanism. A relation is an abstract concept and we do not

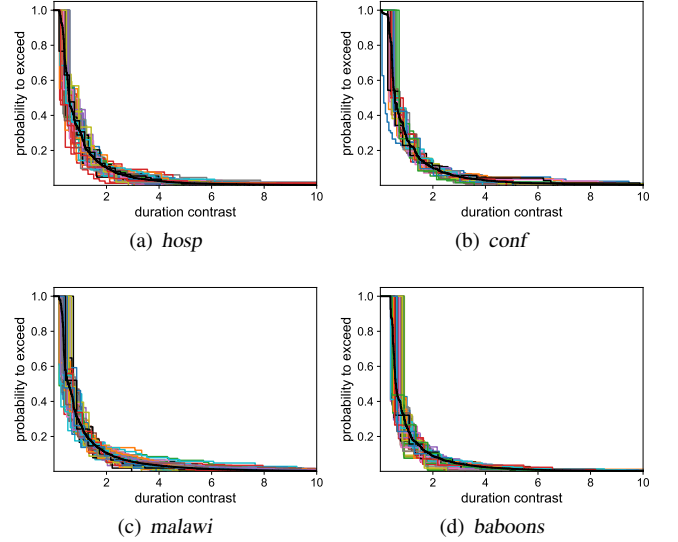


Figure 6. Distributions (p.t.e) of the contact duration contrast for each relation with at least 50 contacts. Each color represent a different distribution. The black line is the combined p.t.e shown in Figure 4.

give in the following a rigorous derivation of our model but rather highlight some of the intuitions that lead to it. Generally speaking a relation is sometimes “tight” and sometimes “loose”. We think about a correlated process where points would gather for some time (the contacts) and then dissociate until the next gathering (encounter). But we are not speaking here about individuals evolving in the physical space who meet sometimes (as in [4, 6]) but about a single point process evolving in an abstract space of “relation”. Since a relation involves two individuals, we will consider a space of dimension 2, challenging this hypothesis in the Discussion. The contrast is a dimensionless quantity; it does not depend on the unit being used for the measurement of the contact duration. If the sensor resolution was different, say  $T=1$  or  $10$  s, the contrast distribution would still look the same since we divide by the mean value (up to finite size effects). This is a signature of a scale-invariant process. We are then led to think about a Levy process or more precisely a Levy flight (or “walk”).

A Levy flight [28, 29] is a continuous random walk process where each increment is isotropic and follows a radial distribution with a p.t.e  $P(> r) = \frac{1}{r^\alpha}$  for  $r > 1$ , where  $0 < \alpha < 2$  is the Levy index. Its particularity is that each step has an infinite variance and that the point-process auto-correlation function is a power-law of the distance between the points (for a precise derivation in a 2D space, see [23, Appendix A]). The stochastic path consists generally in several close points followed by a long jump, with some further possibility to come back near some previous samples.

If we connect all pairs of points that are below some given distance, i.e. set some scale, we obtain a Levy Geometric Graph (LGG) whose properties were studied in [23]. An example is shown on Figure 7.

The graph consists of a set of clusters (connected compo-

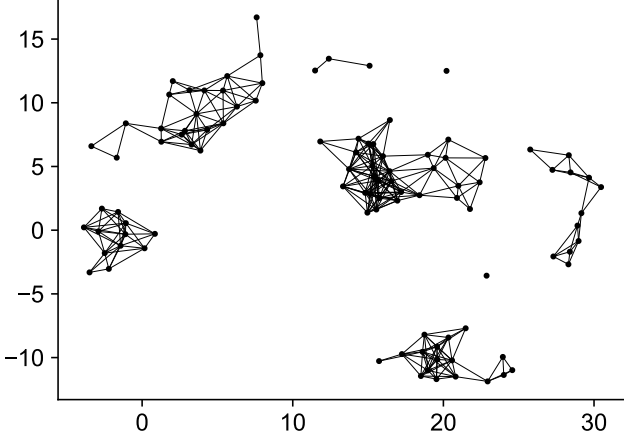


Figure 7. Example of a Levy Geometric Graph ( $N = 100$ ). Vertices are placed at the position of a random Levy flight (here of index  $\alpha = 1$ ) and an edge is created if the distance between 2 vertices is below some distance (the scale, here 3). In our model each cluster represent an interaction between a given pair of individuals, and the size, its duration (in units of the resolution steps).

nents) of various sizes  $C_i$ . It was noticed that the *normalized cluster size*

$$c_i = \frac{N_{clus}}{N} C_i, \quad (4)$$

where  $N_{clus}$  is the total number of clusters and  $N$  the total number of vertices, is scale-invariant, i.e. depends only on  $\alpha$ .

In fact, we notice that since  $N$  is the sum of the clusters size

$$\frac{N_{clus}}{N} = \left( \frac{1}{N_{clus}} \sum_{i=1}^{N_{clus}} C_i \right)^{-1} = \frac{1}{\bar{C}}, \quad (5)$$

the normalized cluster size

$$c_i = \frac{C_i}{\bar{C}} \quad (6)$$

is precisely the cluster size *contrast*.

Intriguingly, the distribution of this contrast variable (Fig.8 of [23]) resembles closely that of Figure 4, which is at the origin of our model.

We then model each relation by a LGG. Each cluster represents an encounter between the pair of individuals and its size the duration of the contact (in units of the resolution step), i.e.,  $t_i = C_i$ .

To run the model, we need to define the size of the graph ( $N$ ) and its scale ( $s$ ).

From the identification of the cluster size to the contact duration

$$N(r) = \sum_{i=1}^{N_{clus}} C_i = \sum_{i=1}^{N_{int}(r)} t_i(r) = w(r) \quad (7)$$

where  $w$  are the weights discussed in Sect. II.

Since we claimed that the cluster size contrast is independent of the scale, we could use a priori any value for it. However this property is only true asymptotically ( $N \rightarrow \infty$ ) and for large scales ( $s \gtrsim 2$ ). In our datasets this is often not the case, so we define it more precisely in the following way. For LGGs, it was shown [23] that the mean number of clusters scales as

$$\frac{N_{clus}}{N} = \frac{A}{s^{\alpha_c}} \quad (8)$$

where  $A$  and  $\alpha_c$  depends only on the Levy index. Their exact values are obtained using LGG simulations. For  $\alpha = 1.1$ , which will be important later, we measure  $A = 0.75$ ,  $\alpha_c = 1.4$  (other values may be found in *SIAppendix, S5*). From eq. (5), the corresponding scale for a given relation is

$$s(r) = [A\bar{t}(r)]^{1/\alpha_c}. \quad (9)$$

In order to account for the quantization of the time measurement (20 s steps) the weights  $w$  and mean-times  $\bar{t}$  are expressed as the number of resolution steps and are thus integers.

Each relation in a dataset is then modeled by an independent Levy graph of size given by eq. (7) and scale given by eq. (9). Since our aim is to model the underlying contrast dynamics, we remove the noise with the  $N_{int}(r) > 50$  cut. LGGs being random graphs, we simulate 10 of them for each relation. Each time we determine the connected components and compute their contrast size ( $C_i/\bar{C}$ ) that we compare to the contact duration contrast measured on the data. We illustrate how the result vary with some values of  $\alpha$  in Figure 8.

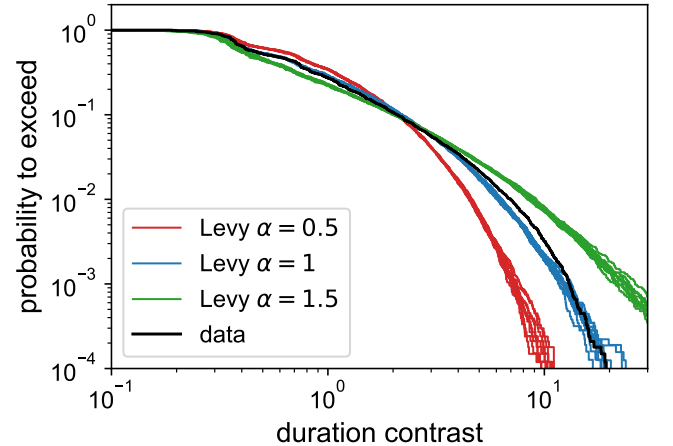


Figure 8. Comparison between the distribution of the duration contrast measured with the *malawi* data (black line) and the cluster-size contrast obtained from 10 simulated LGGs per relation (colored lines) for 3  $\alpha$  values.

The best results are obtained with  $\alpha = 1.1$  and are shown in Figure 9. Although data distributions have similar shapes (they correspond to Figure 4(a)) the size  $N(r)$  and scale  $s(r)$  of the graphs are different for each dataset. The agreement in all the cases is excellent. There are small fluctuations among the random graphs and even the low contrast wiggles are well reproduced.

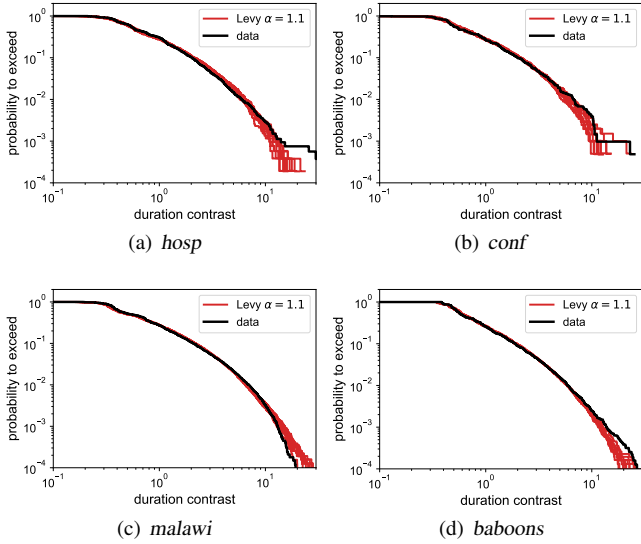


Figure 9. Comparison between the contrast data and our model based on Levy Graphs with an index  $\alpha = 1.1$  on the 4 datasets. By comparing the *malawi* result to Figure 8, we see that an index of  $\alpha = 1.1$  reproduces slightly better the data than  $\alpha = 1$ .

## V. DISCUSSION

We have compared face-to-face interaction data taken in some very different environments; some were recorded in an european hospital or during a scientific conference, others in a small village in Africa. We have also included data on baboons’ interactions originally intended for ethological studies, with the initial thought that they might serve as null-tests for human behavior. We recall that what we call “interaction” here is a face-to-face contact within  $\lesssim 1.5$  m and that lasts at least 20 s. The kind of social exchange during this period is of course very different between humans and animals. For the former it is most probably speaking, while for baboons mostly groom and rest together [21].

Concerning the contacts between individuals, people in the *malawi* dataset interact with a smaller number of persons than in the occidental datasets (hospital and conference). However the interactions are longer, so that the strength of the relations is similar. Baboons on the contrary interact all with each other but for a shorter amount of time. This is limited by the small number of animals (13) and it is not clear how it would extrapolate to a number similar to the human experiments (around 80). This shows the high variability of social face-to-face interactions between humans and also between animals.

Focusing on the temporal aspects of each interaction, it appears that the rate and the mean-time spent together also depends on the social structure (Figure 2). However, once a contact is established, our finding is that the deviation of the contact duration from its mean-value (the contrast) is almost independent of the social structure (Figure 4); the over-duration seems universal, at least on these extremely heterogeneous datasets. But our main finding is that this general behavior is not only valid on the whole population but also at the level

of each individual pair. Since the interactions between the individuals are very different (Sect. II), this indicates that the amount of extra-time spent interacting with a given individual is not strongly affected by the social environment. Once a relation is triggered it has its own dynamics. It can be factored-out from the sociological complicated structure. While one may think that our ability to interact more or less with a given person is related to a common human level of “patience”, the same results for baboons shed doubt on this explanation.

The shape of the contrast distribution mostly comes from the one of the interaction duration (Figure 2). Normalizing it by each relation mean-time (Figure 3(b)) *standardizes* it to a common distribution. This is not a trivial result obtained by dividing by the mean value. When there are many samples ( $N_{int} > 50$ ), the arithmetic mean converges to a single number (the statistical mean) and becomes mostly independent of the individual samples. The contrast distribution then follows essentially a rescaled version of the duration one. If the contact duration were to follow for instance a Poisson distribution, the contrast would have been very different, going to 0 around  $\delta = 4$  (see *SIAppendix, S6*). We recall that the scaling varies with the relation since it depends on each mean-time value.

This “universality” that we find on four very different datasets, holds for face-to-face interactions ( $\lesssim 1.5$  m for at least 20 s) between adults in a mildly dense closed environment. This is observed up to a contrast of about 10. Some differences seem to emerge for larger values but it is difficult to be certain given the data we have at hand. We emphasize that our main finding is that *each* relation follows a similar pattern. This must be put to test with other data. Although they probe a different kind of social interactions, mobile phone communications could show some similar characteristic.

Since there is a clearly observable curvature in Figure 4(a) the contrast distribution does *not* follow a power-law. Neither is it of exponential type. We obtain a good fit to the p.t.e in the  $0.4 < \delta < 10$  region with the following function

$$P(> \delta) = 0.37e^{-0.3\delta}/\delta. \quad (10)$$

We have considered so far the duration of the interactions but not *when* they happen, i.e. the inter-contact or “gap” time. Their contrast could also show some universality. This is not the case as shown in Figure 10. The contrast of the inter-contact time depends on the sociological environment.

Some models that describe face-to-face interactions do exist. They are either based on a mechanism of preferential attachment to groups of individuals [2, 3] or on a (standard) random walk that describes the physical displacements that must be biased [4–6]. They all contain parameters to be adjusted, while our model has none once  $\alpha$  is fixed to 1.1. Whether the agent-based models can reproduce the contrast for *each* relation, in particular on the *malawi* and *baboons* datasets, remains to be proven. But the essential difference with our model is that they are all *agent-based*, trying to reproduce a collective behavior from each individual one, while our approach is to model the very concept of *relation*. In some aspects, agent-based models have a richer phenomenology since they can predict the structure of interactions between individuals while we use as an input the distributions of the interac-

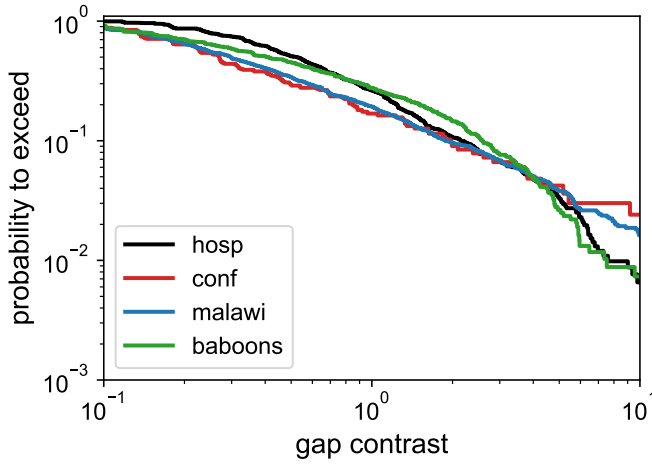


Figure 10. Distributions of the contrasts of the gap-time (inter-contact duration) on our datasets. To avoid the long night breaks, we show results for a single day.

tion rates  $N_{int}(r)$  and the mean-time  $\bar{t}(r)$ . Agent-based models could then be used to define those values, handling the detail of the relation within our model, i.e separating the “sociological” part from the “universal” one.

Power-law distributions are ubiquitous in the field of human interactions. They are observed for instance in the delay to answer e-mails [30], in human travels [31], or on the time we spend at a given location [1]. Interestingly, the measured power slopes are always around 1. But they are obtained very differently, by fitting 1D temporal data assuming a power-law distribution. In our model the Levy index  $\alpha$  characterizes a random-walk in 2D space, and does not lead to power-law distributions.

The idea behind using Levy graphs is the following. In a particular relation, the duration of the contact has no particular scale; it essentially depends on our free-will. However due to social constraints, especially for work-related activities, there exist some implicit limitation on the length of each discussion so that the mean-time in each relation does not drift too much (no one spends the full day talking with the same person). This sets a scale, that can be different for each pair according to the level both participants enjoy interacting. Levy graphs precisely describe what happens when we apply a scale (here related to  $\bar{t}$ , see eq. (9)) to a scale-free process (the time during which we communicate). What appears immediately when studying LGGs, is that their clusters have a very specific size distribution. In particular their contrast is similar to the one obtained for the contact durations. A closer examination revealed us that this agreement was in fact excellent and that all the data can be reproduced very accurately with a unique Levy index,  $\alpha = 1.1$ . The main argument in favor of this model is then its success for matching non-trivial data with a single parameter.

One may ask what the nature of the “space of relation” is. We note that in social networks, the “space of relations” is also an abstract concept. It is only used for representation, the real mathematical object being the graph itself. A differ-

ence is that a Levy flight requires a *metric* space to perform the steps. However the distance is dimensionless. Indeed a genuine Levy flight has a minimal step size  $r_0$ . When connecting points, the linking length  $L$  has the same dimension. What we call the scale is  $s = L/r_0$ . In our model, without loss of generality, we have assumed  $r_0 = 1$ . In Figure 7 we could have scaled as well the axes by a factor 2 using  $r_0 = 2$ . As in social networks, what really matters is the graph itself not its representation.

The 2D space is dictated by the data. We have checked that using a Levy walk in a higher dimension space, the agreement with the data gets worse (SIAppendix, S7). This is maybe due to the fact that a relation involves two agents. However this then raises another question. In a low dimensional space, one cannot consider the Levy process as solely consisting of a few local steps followed by a long jump leading to a new cluster. There is a non-negligible probability (about 20% for  $\alpha = 1$ , see [23]) that the walker comes back to a previous set of points and contributes to the cluster size, thus to the duration of the contact in our model. Increasing the dimension, the return probability decreases and the contrast p.t.e converges to  $e^{-\delta}$ , which is not observed on data (eq. (10)). The meaning of this return-probability, which is not a physical displacement in the real space, remains to be understood.

Levy flights belong to a very peculiar class of correlated point-processes without any mean-density but a power-law autocorrelation function of the form  $\xi(r) \propto 1/r^{2-\alpha}$  (in 2D) where  $r > 1$  is the dimensionless distance in the relation space. Such an autocorrelation gives rise to scale-invariance since for any  $b$  we have  $\xi(br) \propto \xi(r)$ . The process looks (statistically) the same at any scale. This translates for Levy graphs into the fact that the cluster-size contrast is scale-invariant. This is only true for a large number of samples and for a scale above  $\geq 2$ . Both could be achieved with an experiment with a finer timing resolution, since the time units ( $t_i$  and  $\bar{t}$ ) would increase. A prediction from our model is that the contrast distribution would not show anymore the wiggles at low contrast (SIAppendix, S8).

In classical random geometric graphs, based on uncorrelated points, a geometric phase transition appears when increasing the scale; most points end up belonging to a single cluster, the giant component. In 2D this happens around a mean degree of 4.5 [32]. This is not the case for Levy graphs that escape this capture due to the long jumps. This property leads in our case to the fact that clusters, i.e. encounters between two individuals, always exist whatever the scale is. It is a necessary condition for a random-graph based model, since otherwise, by increasing the resolution of the instrument the size and scale (see eq. (7), eq. (9)) would also increase, leading to a single very long interaction.

Finally, Levy flights have been much discussed in the context of movements of foraging animals [33] and were also observed in some human communities practicing hunting [34] or looking for resources [35]. Whether they really represent the optimal random-search strategy has been hotly debated [36–40], but they are certainly advantageous in several aspects [41–43]. This suggests that we may also be searching for something in a face-to-face relation.



## CONFLICT OF INTEREST DISCLOSURE

The authors declare no conflict of interest.

## SOFTWARE AVAILABILITY

The (python3) scripts used to produce the results are available from <https://gitlab.in2p3.fr/plaszczyni/coll> (the entry point is `gtAgg.py`).

## DATA AVAILABILITY

All data are available from the *sociopatterns* web site [www.sociopatterns.org](http://www.sociopatterns.org)

## ACKNOWLEDGEMENTS

The authors thank Basile Grammaticos and Mathilde Badoual for fruitful discussions and corrections on the manuscript. The graph-related computations and Figure 1 were performed using graph-tools : <https://graph-tool.skewed.de>

- 
- [1] Chaoming Song, Tal Koren, Pu Wang, and Albert-László Barabási. Modelling the scaling properties of human mobility. *Nature Physics*, 6(10):818–823, 2010. ISSN 1745-2473, 1745-2481. doi:10.1038/nphys1760.
  - [2] Juliette Stehle, Alain Barrat, and Ginestra Bianconi. Dynamical and bursty interactions in social networks. *Physical Review E*, 81(3):035101, March 2010. ISSN 1539-3755, 1550-2376. doi:10.1103/PhysRevE.81.035101.
  - [3] Kun Zhao, Juliette Stehle, Ginestra Bianconi, and Alain Barrat. Social network dynamics of face-to-face interactions. *Physical Review E*, 83(5):056109, May 2011. ISSN 1539-3755, 1550-2376. doi:10.1103/PhysRevE.83.056109.
  - [4] Michele Starnini, Andrea Baronchelli, and Romualdo Pastor-Satorras. Modeling Human Dynamics of Face-to-Face Interaction Networks. *Physical Review Letters*, 110(16):168701, April 2013. ISSN 0031-9007, 1079-7114. doi:10.1103/PhysRevLett.110.168701.
  - [5] Vedran Sekara, Arkadiusz Stopczynski, and Sune Lehmann. Fundamental structures of dynamic social networks. *Proceedings of the National Academy of Sciences*, 113(36):9977–9982, September 2016. ISSN 0027-8424, 1091-6490. doi:10.1073/pnas.1602803113.
  - [6] Marco Antonio Rodríguez Flores and Fragkiskos Papadopoulos. Similarity Forces and Recurrent Components in Human Face-to-Face Interaction Networks. *Physical Review Letters*, 121(25):258301, December 2018. ISSN 0031-9007, 1079-7114. doi:10.1103/PhysRevLett.121.258301.
  - [7] Hugo Barbosa, Marc Barthelemy, Gourab Ghoshal, Charlotte R. James, Maxime Lenormand, Thomas Louail, Ronaldo Menezes, José J. Ramasco, Filippo Simini, and Marcello Tomasini. Human mobility: Models and applications. *Physics Reports*, 734:1–74, March 2018. doi:10.1016/j.physrep.2018.01.001. URL <https://doi.org/10.1016/j.physrep.2018.01.001>.
  - [8] Pan Hui, Augustin Chaintreau, James Scott, Richard Gass, Jon Crowcroft, and Christophe Diot. Pocket switched networks and human mobility in conference environments. In *Proceeding of the 2005 ACM SIGCOMM Workshop on Delay-tolerant Networking - WDTN '05*, pages 244–251, Philadelphia, Pennsylvania, USA, 2005. ACM Press. ISBN 978-1-59593-026-2. doi:10.1145/1080139.1080142.
  - [9] A. Scherrer, P. Borgnat, E. Fleury, J.-L. Guillaume, and C. Robardet. Description and simulation of dynamic mobility networks. *Computer Networks*, 52(15):2842–2858, 2008. ISSN 13891286. doi:10.1016/j.comnet.2008.06.007. URL <https://linkinghub.elsevier.com/retrieve/pii/S138912860800193X>.
  - [10] Ciro Cattuto, Wouter Van den Broeck, Alain Barrat, Vittoria Colizza, Jean-François Pinton, and Alessandro Vespignani. Dynamics of Person-to-Person Interactions from Distributed RFID Sensor Networks. *PLoS ONE*, 5(7):e11596, July 2010. ISSN 1932-6203. doi:10.1371/journal.pone.0011596.
  - [11] A. Barrat, C. Cattuto, A.E. Tozzi, P. Vanhems, and N. Voirin. Measuring contact patterns with wearable sensors: Methods, data characteristics and applications to data-driven simulations of infectious diseases. *Clinical Microbiology and Infection*, 20(1):10–16, January 2014. ISSN 1198743X. doi:10.1111/1469-0691.12472.
  - [12] Juliette Stehlé, Nicolas Voirin, Alain Barrat, Ciro Cattuto, Vittoria Colizza, Lorenzo Isella, Corinne Régis, Jean-François Pinton, Nagham Khanafer, Wouter Van den Broeck, and Philippe Vanhems. Simulation of an SEIR infectious disease model on the dynamic contact network of conference attendees. *BMC Medicine*, 9(1):87, December 2011. ISSN 1741-7015. doi:10.1186/1741-7015-9-87.
  - [13] Lorenzo Isella, Juliette Stehlé, Alain Barrat, Ciro Cattuto, Jean-François Pinton, and Wouter Van den Broeck. What's in a crowd? Analysis of face-to-face behavioral networks. *Journal of Theoretical Biology*, 271(1):166–180, December 2010. ISSN 00225193. doi:10.1016/j.jtbi.2010.11.033.
  - [14] Michele Starnini, Andrea Baronchelli, Alain Barrat, and Romualdo Pastor-Satorras. Random walks on temporal networks. *Physical Review E*, 85(5):056115, May 2012. ISSN 1539-3755, 1550-2376. doi:10.1103/PhysRevE.85.056115.
  - [15] Mathieu Génois, Christian L. Vestergaard, Julie Fournet, André Panisson, Isabelle Bonmarin, and Alain Barrat. Data on face-to-face contacts in an office building suggest a low-cost vaccination strategy based on community linkers. *Network Science*, 3(3):326–347, September 2015. ISSN 2050-1242, 2050-1250. doi:10.1017/nws.2015.10.
  - [16] Philippe Vanhems, Alain Barrat, Ciro Cattuto, Jean-François Pinton, Nagham Khanafer, Corinne Régis, Byeul-a Kim, Brigitte Comte, and Nicolas Voirin. Estimating Potential Infection Transmission Routes in Hospital Wards Using Wearable Proximity Sensors. *PLoS ONE*, 8(9):e73970, September 2013. ISSN 1932-6203. doi:10.1371/journal.pone.0073970.
  - [17] Julie Fournet and Alain Barrat. Contact Patterns among High School Students. *PLoS ONE*, 9(9):e107878, September 2014.

- ISSN 1932-6203. doi:10.1371/journal.pone.0107878.
- [18] Rossana Mastrandrea, Julie Fournet, and Alain Barrat. Contact patterns in a high school: A comparison between data collected using wearable sensors, contact diaries and friendship surveys. *PLoS ONE*, 10(9):e0136497, 09 2015. doi: 10.1371/journal.pone.0136497. URL <http://dx.doi.org/10.1371%2Fjournal.pone.0136497>.
- [19] Moses C Kiti, Michele Tizzoni, Timothy M Kinyanjui, Dorothy C Koech, Patrick K Munywoki, Milosch Meriac, Luca Cappa, André Panisson, Alain Barrat, Ciro Cattuto, and D James Nokes. Quantifying social contacts in a household setting of rural Kenya using wearable proximity sensors. *EPJ Data Science*, 5(1):21, December 2016. ISSN 2193-1127. doi: 10.1140/epjds/s13688-016-0084-2.
- [20] Laura Ozella, Daniela Paolotti, Guilherme Lichand, Jorge P. Rodríguez, Simon Haenni, John Phuka, Onicio B. Leal-Neto, and Ciro Cattuto. Using wearable proximity sensors to characterize social contact patterns in a village of rural Malawi. *EPJ Data Science*, 10(1):46, December 2021. ISSN 2193-1127. doi: 10.1140/epjds/s13688-021-00302-w.
- [21] Gelardi et al. Measuring social networks in primates: Wearable sensors versus direct observations. <https://royalsocietypublishing.org/doi/epdf/10.1098/rspa.2019.0737>, 2020.
- [22] Alain Barrat and Ciro Cattuto. Face-to-Face Interactions. In Bruno Gonçalves and Nicola Perra, editors, *Social Phenomena*, pages 37–57. Springer International Publishing, Cham, 2015. ISBN 978-3-319-14010-0 978-3-319-14011-7. doi: 10.1007/978-3-319-14011-7\_3.
- [23] S. Plaszczynski, G. Nakamura, C. Deroulers, B. Grammaticos, and M. Badoual. Levy geometric graphs. *Phys. Rev. E*, 105: 054151, May 2022. doi:10.1103/PhysRevE.105.054151. URL <https://link.aps.org/doi/10.1103/PhysRevE.105.054151>.
- [24] Note1. here and in the following, we will only consider complete (24 h) day periods.
- [25] Mathieu Génois and Alain Barrat. Can co-location be used as a proxy for face-to-face contacts? *EPJ Data Science*, 7(1): 11, May 2018. ISSN 2193-1127. doi:10.1140/epjds/s13688-018-0140-1. URL <https://doi.org/10.1140/epjds/s13688-018-0140-1>.
- [26] M. E. J. Newman. Power laws, Pareto distributions and Zipf’s law. *Contemporary Physics*, 46(5):323–351, September 2005. ISSN 0010-7514, 1366-5812. doi: 10.1080/00107510500052444.
- [27] A. Barrat, M. Barthélemy, R. Pastor-Satorras, and A. Vespignani. The architecture of complex weighted networks. *Proceedings of the National Academy of Sciences*, 101(11): 3747–3752, 2004. ISSN 0027-8424, 1091-6490. doi: 10.1073/pnas.0400087101.
- [28] Benoit Mandelbrot. ”sur un modèle décomposable d’univers hiérarchisé: déduction des corrélations galactiques sur la sphère céleste.”. *Comptes Rendus (Paris)*, 280A:1551–1554, 1975. URL [https://users.math.yale.edu/mandelbrot/web\\_pdfs/comptes\\_rendus\\_79.pdf](https://users.math.yale.edu/mandelbrot/web_pdfs/comptes_rendus_79.pdf).
- [29] Benoit Mandelbrot. *The Fractal Geometry of Nature*. Freeman, San Francisco, 1983.
- [30] Albert-László Barabási. The origin of bursts and heavy tails in human dynamics. *Nature*, 435(7039):207–211, 2005. ISSN 0028-0836, 1476-4687. doi:10.1038/nature03459.
- [31] D. Brockmann, L. Hufnagel, and T. Geisel. The scaling laws of human travel. *Nature*, 439(7075):462–465, January 2006. ISSN 0028-0836, 1476-4687. doi:10.1038/nature04292.
- [32] Jesper Dall and Michael Christensen. Random geometric graphs. *Phys. Rev. E*, 66(1):016121, July 2002. ISSN 1063-651X, 1095-3787. doi:10.1103/PhysRevE.66.016121. URL <https://link.aps.org/doi/10.1103/PhysRevE.66.016121>.
- [33] Gandhimohan. M. Viswanathan, Marcos G. E. da Luz, Ernesto P. Raposo, and H. Eugene Stanley. *The Physics of Foraging: An Introduction to Random Searches and Biological Encounters*. Cambridge University Press, 2011. doi: 10.1017/CBO9780511902680.
- [34] David A. Raichlen, Brian M. Wood, Adam D. Gordon, Audax Z. P. Mabulla, Frank W. Marlowe, and Herman Pontzer. Evidence of Lévy walk foraging patterns in human hunter–gatherers. *Proceedings of the National Academy of Sciences*, 111(2):728–733, January 2014. ISSN 0027-8424, 1091-6490. doi:10.1073/pnas.1318616111.
- [35] Andy Reynolds, Eliane Ceccon, Cristina Baldauf, Tassia Karina Medeiros, and Octavio Miramontes. Lévy foraging patterns of rural humans. *PLOS ONE*, 13(6):e0199099, June 2018. ISSN 1932-6203. doi:10.1371/journal.pone.0199099.
- [36] G. M. Viswanathan, Sergey V. Buldyrev, Shlomo Havlin, M. G. E. da Luz, E. P. Raposo, and H. Eugene Stanley. Optimizing the success of random searches. *Nature*, 401(6756): 911–914, October 1999. ISSN 0028-0836, 1476-4687. doi: 10.1038/44831.
- [37] G.M. Viswanathan, E.P. Raposo, and M.G.E. da Luz. Lévy flights and superdiffusion in the context of biological encounters and random searches. *Physics of Life Reviews*, 5(3):133–150, September 2008. ISSN 15710645. doi: 10.1016/j.plrev.2008.03.002.
- [38] E P Raposo, S V Buldyrev, M G E da Luz, G M Viswanathan, and H E Stanley. Lévy flights and random searches. *Journal of Physics A: Mathematical and Theoretical*, 42(43):434003, October 2009. ISSN 1751-8113, 1751-8121. doi:10.1088/1751-8113/42/43/434003.
- [39] Alex James, Michael J. Plank, and Andrew M. Edwards. Assessing Lévy walks as models of animal foraging. *Journal of The Royal Society Interface*, 8(62):1233–1247, September 2011. ISSN 1742-5689, 1742-5662. doi: 10.1098/rsif.2011.0200.
- [40] Andy Reynolds. Liberating Lévy walk research from the shackles of optimal foraging. *Physics of Life Reviews*, 14:59–83, September 2015. ISSN 15710645. doi: 10.1016/j.plrev.2015.03.002.
- [41] E. P. Raposo, Sergey V. Buldyrev, M. G. E. da Luz, M. C. Santos, H. Eugene Stanley, and G. M. Viswanathan. Dynamical Robustness of Lévy Search Strategies. *Physical Review Letters*, 91(24):240601, December 2003. ISSN 0031-9007, 1079-7114. doi:10.1103/PhysRevLett.91.240601.
- [42] Michael A. Lomholt, Koren Tal, Ralf Metzler, and Klafter Joseph. Lévy strategies in intermittent search processes are advantageous. *Proceedings of the National Academy of Sciences*, 105(32):11055–11059, August 2008. ISSN 0027-8424, 1091-6490. doi:10.1073/pnas.0803117105.
- [43] Nicolas E. Humphries and David W. Sims. Optimal foraging strategies: Lévy walks balance searching and patch exploitation under a very broad range of conditions. *Journal of Theoretical Biology*, 358:179–193, October 2014. ISSN 00225193. doi: 10.1016/j.jtbi.2014.05.032.

“How much do we stand our fellows?  
A universal behavior in face-to-face relations”

## Supplementary Information

S. Plaszczynski and G. Nakamura

February 14, 2023

### Contents

<b>S1 Main results</b>	<b>2</b>
<b>S2 Other datasets</b>	<b>3</b>
<b>S3 Number of interactions</b>	<b>4</b>
<b>S4 Simulations without a minimal number of interactions</b>	<b>5</b>
S4.1 Combined contrast . . . . .	5
S4.2 Contrast per relation . . . . .	5
<b>S5 Number of clusters in Levy graphs</b>	<b>9</b>
<b>S6 Poisson duration</b>	<b>10</b>
<b>S7 Dimension above 2</b>	<b>10</b>
<b>S8 Effect of the time resolution</b>	<b>11</b>

# S1 Main results

There are 2 major results in this work.

The first one concerns the duration of face-to-face contacts between *each* pair of individuals. Although the mean value may vary, the *deviation* from this mean value is very similar in several very different social contexts. As in other fields of physics (e.g cosmology) we call this over/under-duration the duration *contrast*. It is a dimensionless value that describes how much given an interaction is longer or shorter than its usual (mean) time and can be expressed in percents. By construction its mean value is 1.

To remove some statistical noise, we only use data where there is a sufficient number of interactions (samples)  $N_{int}$ . Since the duration distribution is heavy-tailed we use a large minimal value of 50.

Figure 1 (a) shows how the distribution of the duration of contacts and how it changes when computing the contrast in (b). Both use the  $N_{int} > 50$  cut.

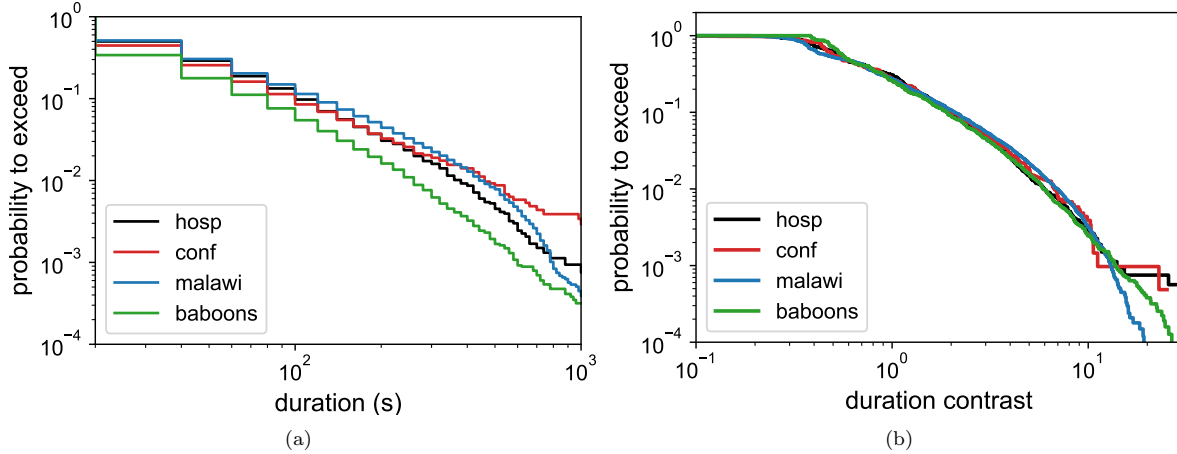


Figure 1: (a) distributions (p.t.e) of the durations of contact and (b) contrast durations on the 4 datasets. The cut  $N_{int} > 50$  is used for both.

The second major result is the spectacular agreement of our model with the data. We recall how the model proceeds:

1. on a given dataset we loop on all the pair of contacts that were registered (“relation”,  $r$ ) over the full duration of the experiment. We keep only timelines where there are at least 50 intervals of interaction.
2. for a given pair ( $r$ ) we determine its mean duration value :  $\bar{t}(r)$ .
3. we draw 10 random Levy graph with  $\alpha = 1.1$  for each relation  $r$ . Their size is given by the weight  $N(r) = w(r)$ , and their scale (linking length) by  $s(r) = (A\bar{t}(r))^{1/\alpha_c}$ , where  $A \simeq 1$  and  $\alpha_c \simeq \alpha$  are determined from LGG simulations and are given for some  $\alpha$  values in Sect. S5. Times ( $w$  and  $\bar{t}$ ) are expressed as a raw number of resolution steps (20 s) and are thus integers.

Although the contrast data are very similar (Figure 1 (b)) we show the results on the 4 datasets since the sizes  $N(r)$  and scales  $s(r)$  are different in each case.



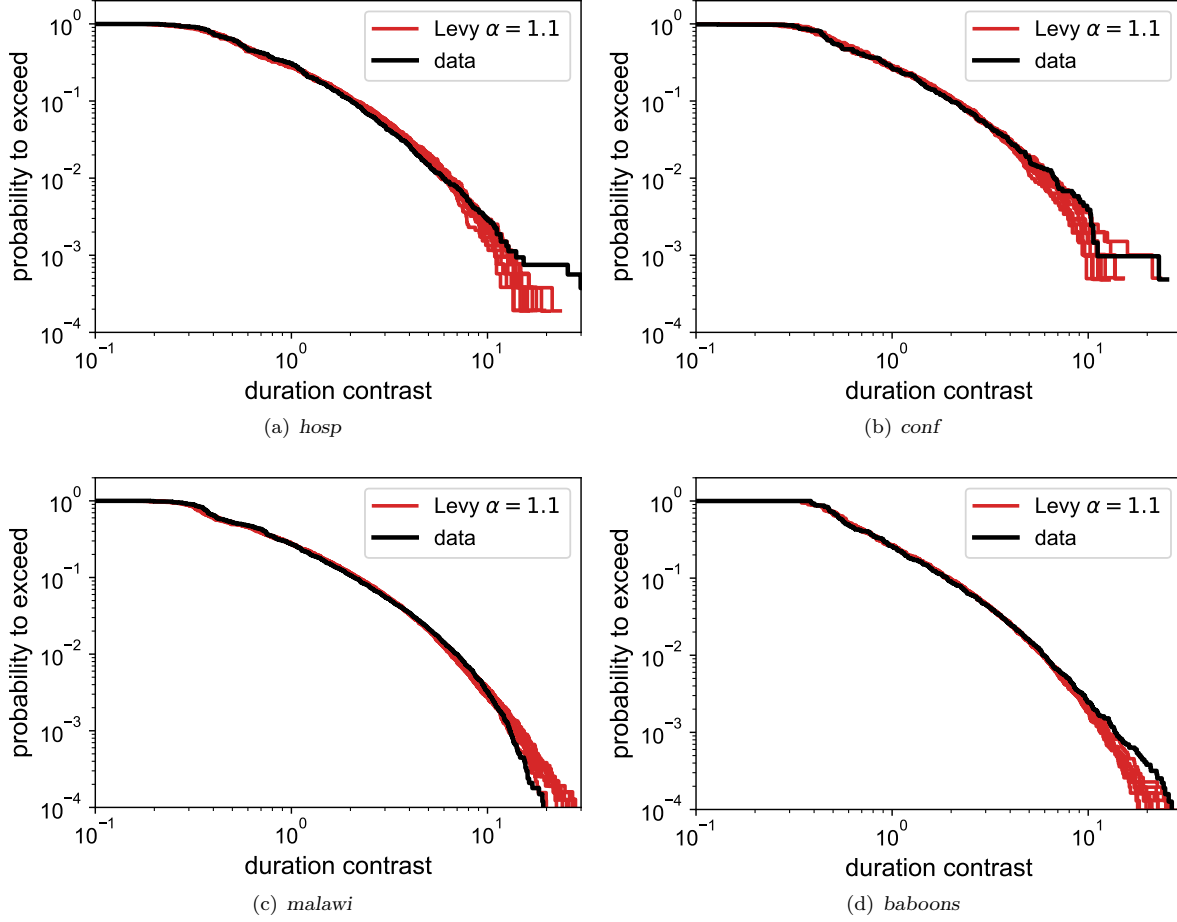


Figure 2: (a) distributions (p.t.e) of the durations of contact and (b) contrast durations on the 4 datasets. The cut  $N_{int} > 50$  is used for both.

## S2 Other datasets

Although in our work we have focused on the sociologically different datasets, we have also looked at some other data provided by the *sociopattern* collaboration.

1. *conf2*: these are data taken at another conference (SFHH,[1, 2]) with  $\simeq 380$  participants for 2 days.
2. *office*: data taken at an office (Intitut de Veille Sanitaire near Paris, [3, 4]) with about 165 participants for 10 days.
3. *highschool*: data from a french high-school, near Marseille [5, 6]. About 300 participants for 4 days

As in Sect. S1 we show how using the contrast standardizes the contact durations on Figure 3 on these new datasets; for comparison we also included the previous *conf* result and still use the  $N_{int} > 50$  cut.

The contrast distributions are similar to the results presented in the paper, and differences are barely noticeable in a linear representation.

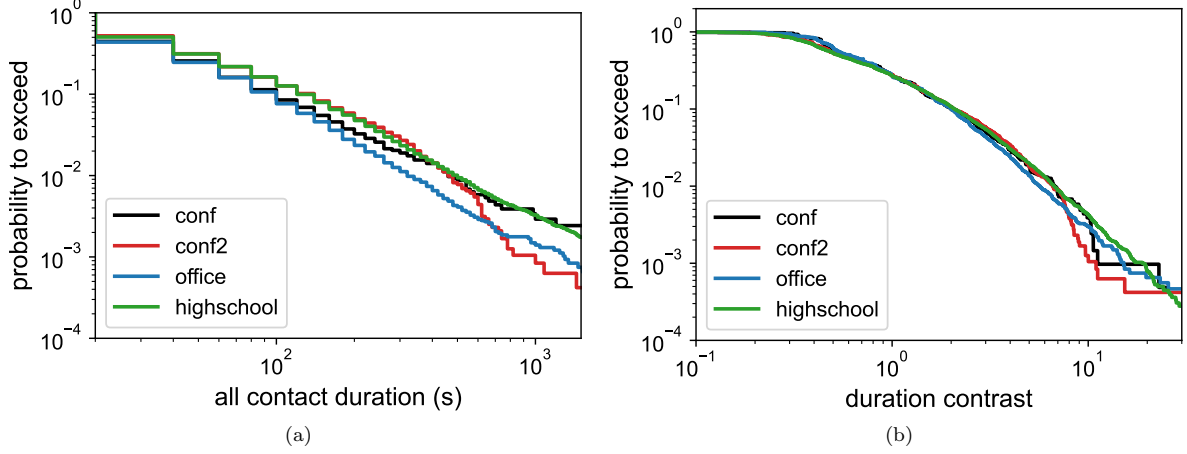


Figure 3: (a) distributions (p.t.e) of the durations of contact and (b) contrast durations for 3 other datasets.

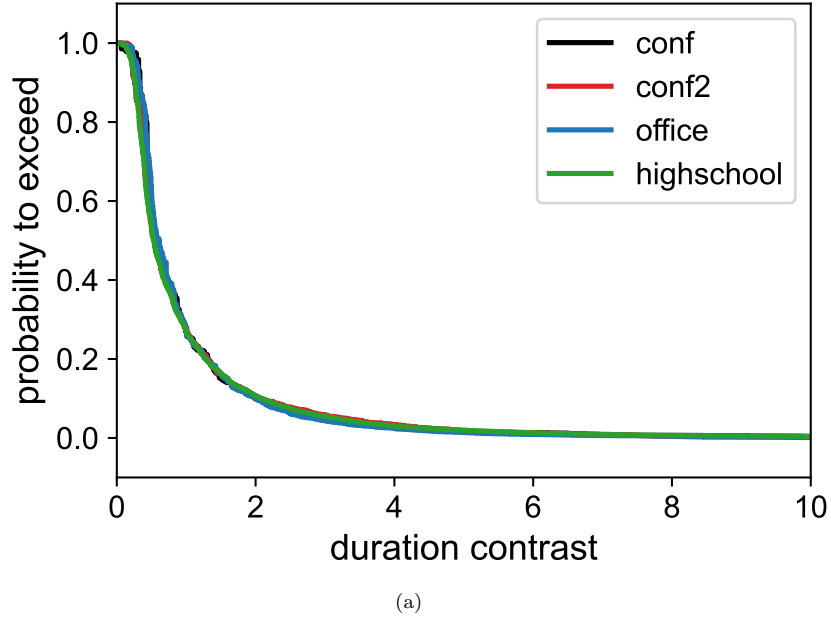


Figure 4: Same as Figure 3 (b) in linear scale.

### S3 Number of interactions

To compute a mean value one (traditionally) invokes the central limit theorem and compute a reliable arithmetic mean with  $\simeq 20$  samples . However the contact duration distribution is very wide (Figure 1(a)) so we prefer to increase that value to  $N_{int} > 50$  before computing the contrast, still keeping a reasonable number of timelines in each case. We may use a lower cutoff and the contrasts distributions are still similar(Figure 5) . But we have added some noisy samples. Note that this value of 50 is only dictated by the data limit data-taking period. Had we a really long period, the mean interaction times between each pair would be well known and this cut would be not necessary.

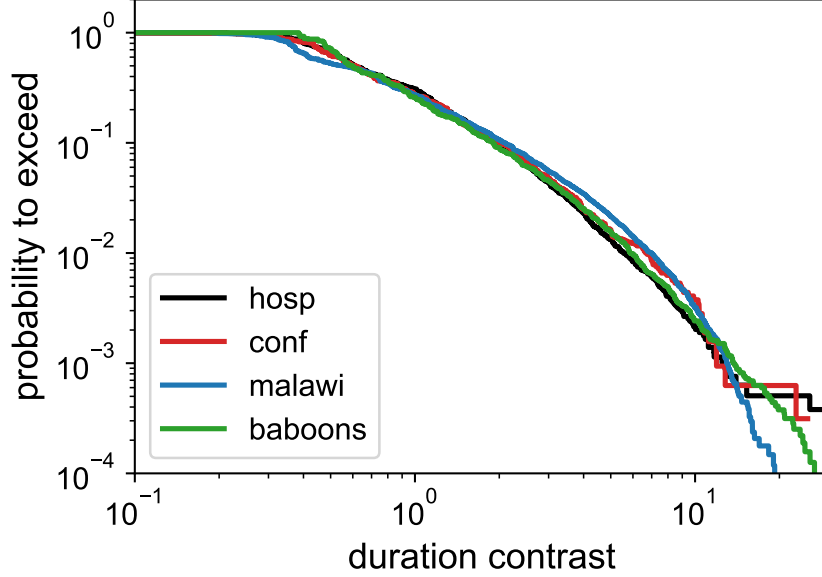


Figure 5: Distribution of the contrast durations on the 4 datasets using a  $N_{int}(r) > 30$  cut.

## S4 Simulations without a minimal number of interactions

### S4.1 Combined contrast

We have shown in the manuscript how to reproduce the noise present on the data for all  $N_{int}$  values on the *conf* dataset in Section 3. Figure 6 shows the results for the other datasets. We reproduce all the data, using only a small fraction of the timelines (the ones with  $N_{int} > 50$  which represents respectively ).

### S4.2 Contrast per relation

In the previous section, the duration (and contrast) of all contacts are combined on Figure 6 in the sense the contrast of each relation are mixed together. We now consider each relation and show its contrast p.t.e with different colors. The timelines are noisy since we do not use any minimal number of steps ( $N_{int}$ ). The *baboons* result is less noisy but this is only due to the fact that the timelines have more samples due to the longer data-taking period (26 days).

We then perform the same simulations than described in the manuscript, but this time on each relation individually. Once again only the global shape of the contrast obtained with the  $N_{int} > 50$  cut (i.e. Figure 1(b)) is used to draw the random numbers. The results are shown on Figure 8. They resembles closely the data (Figure 7). This confirms that the shape and spread observed on data (Figure 7) can be reproduced using only the cleaned Figure 1 distribution ( $N_{int}(r) > 50$  and statistical fluctuations (on the mean) due to the limited size statistics.

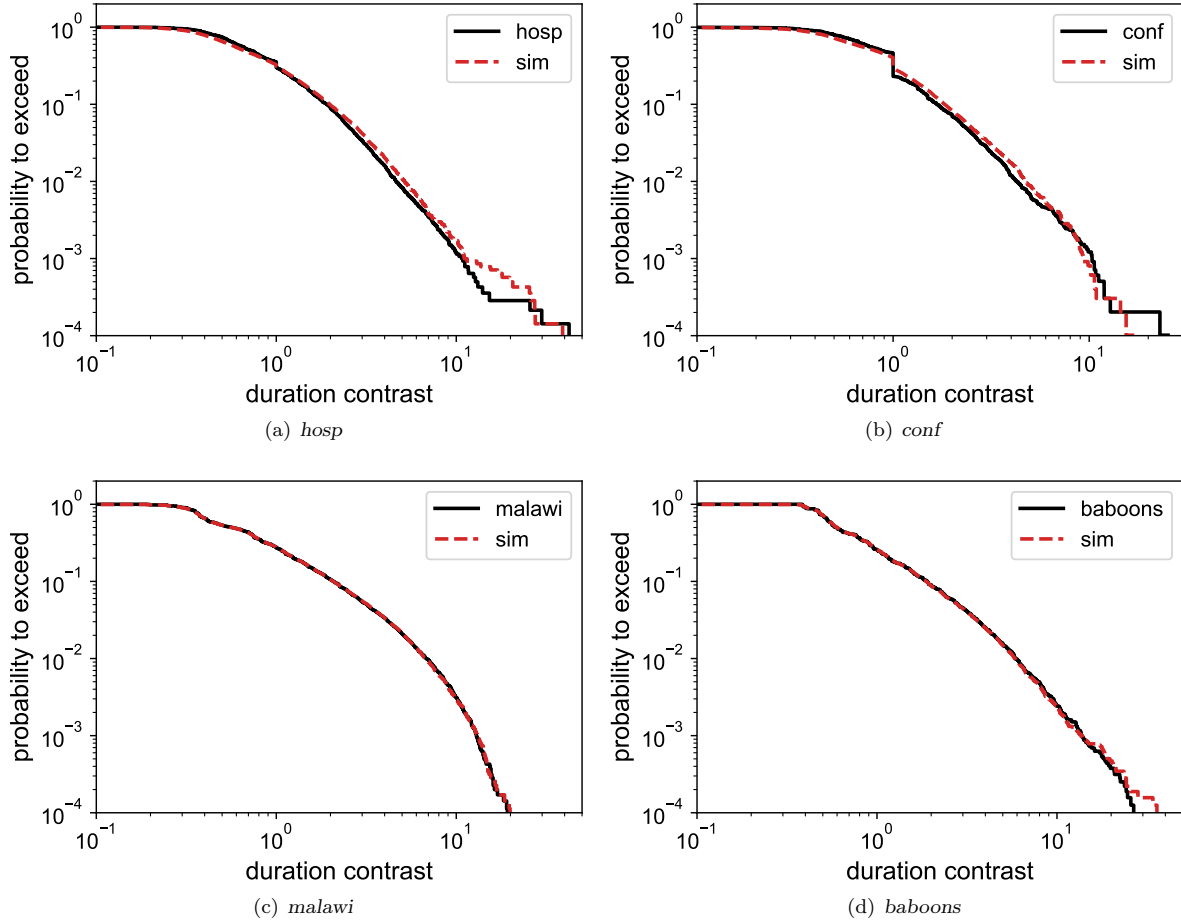


Figure 6: Results of the simulations described in the manuscript (Sect 3) without using a cut on  $N_{int}$  for all the datasets.



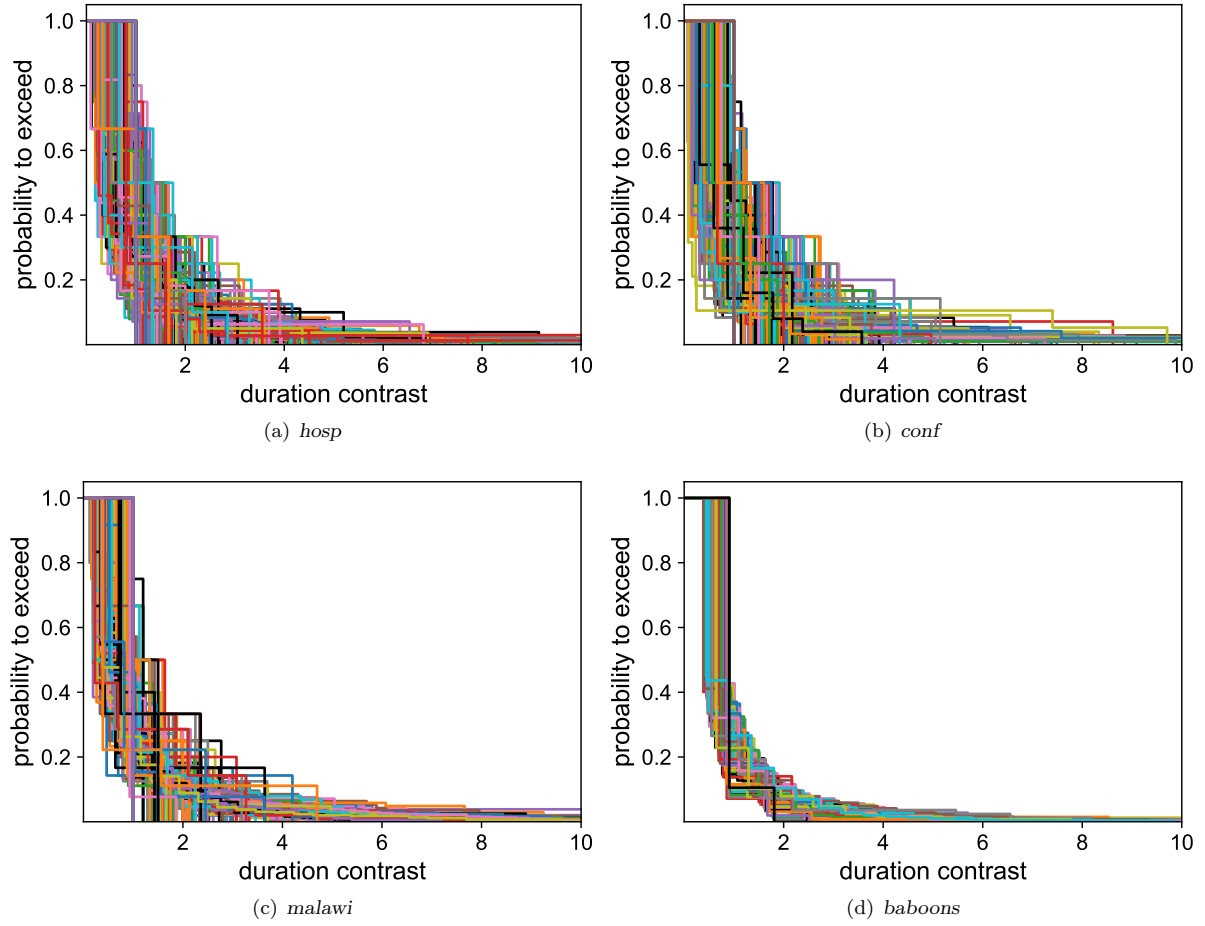


Figure 7: Contrast distributions per relation measured on the data without any  $N_{int}$  cut. Each color represents a different relation timeline.

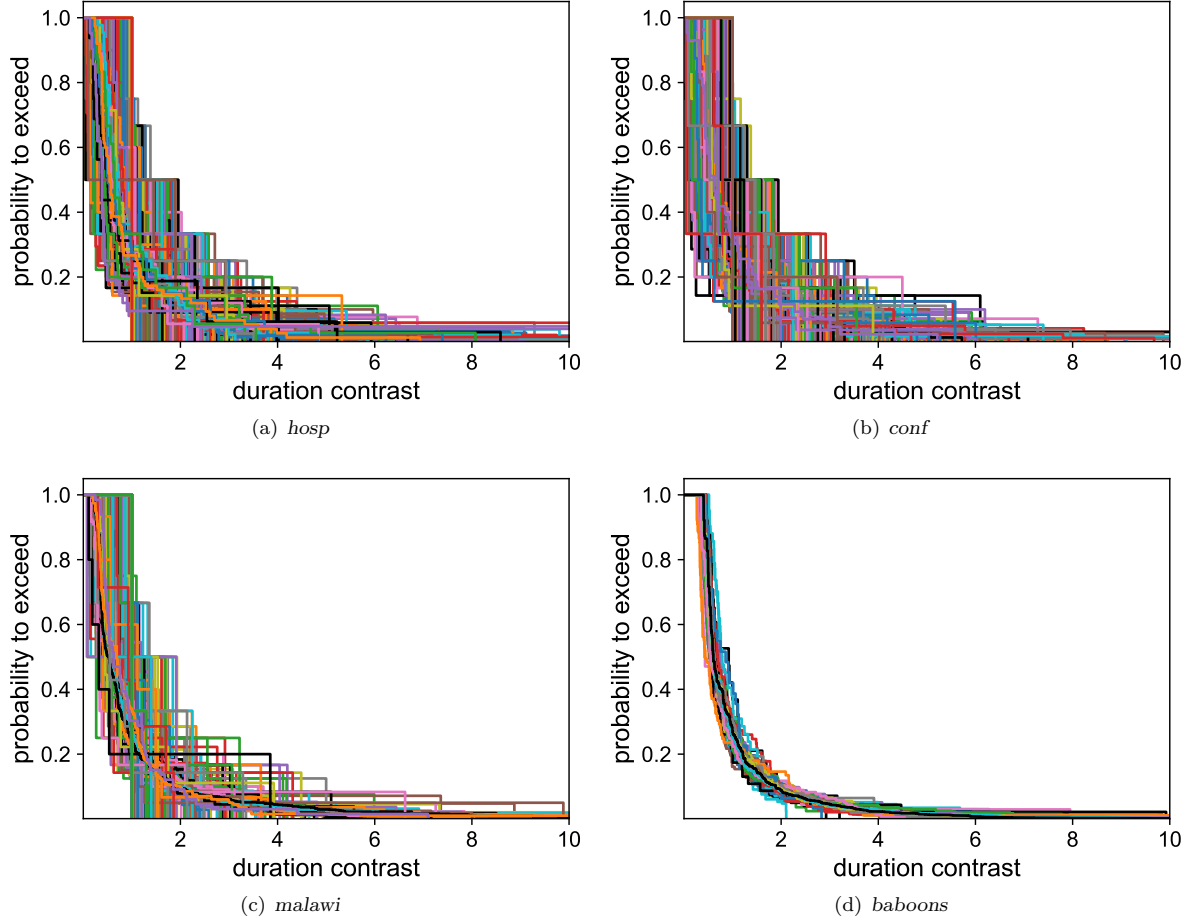


Figure 8: Results of the simulations described in the manuscript (Sect 3) for each relation (colored curves) without using a cut on  $N_{int}$  for all the datasets.

## S5 Number of clusters in Levy graphs

As shown in [7], the mean fraction of clusters follows a power-law function of the scale with a relatively small spread among realizations

$$\frac{N_{clus}}{N} = \frac{A}{s^{\alpha_c}} \quad (1)$$

$A$  and  $\alpha_c$  are determined using 1000 realizations of LGGs for a fixed  $\alpha$  value and varying the scale  $s$  between 1 and 10. Figure 9 shows the results and the power-law fits. The resulting parameters are given in Table 1

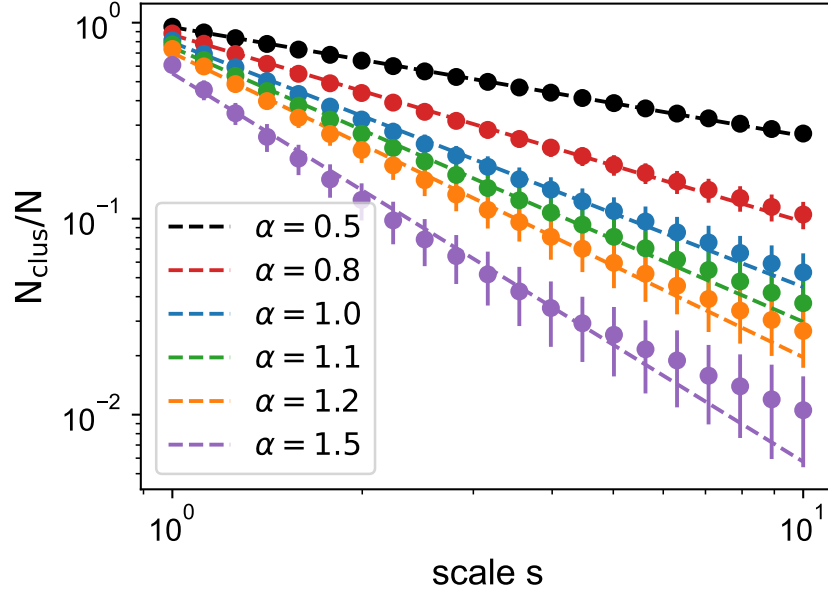


Figure 9: Mean fraction of clusters as a function of the scale as determined from LGG simulations for several  $\alpha$  values. Dashed lines represent the best power-law fits.

$\alpha$	$A$	$\alpha_c$
0.50	$0.95 \pm 0.01$	$0.56 \pm 0.01$
0.80	$0.87 \pm 0.02$	$0.95 \pm 0.02$
1.00	$0.79 \pm 0.02$	$1.25 \pm 0.04$
1.10	$0.75 \pm 0.02$	$1.40 \pm 0.05$
1.20	$0.70 \pm 0.03$	$1.55 \pm 0.06$
1.50	$0.55 \pm 0.03$	$1.98 \pm 0.09$

Table 1: Coefficients of eq. (1) fitted from the 2D LGG simulations (Figure 9) for various  $\alpha$  values.

## S6 Poisson duration

Dividing my mean-values does not necessarily lead to distributions of the Figure 1 kind. We illustrate that feature by computing the contrast using Poisson-distributed durations. To this purpose we use the *hosp* data to obtain the  $\bar{t}(r)$  values for each relation; we then draw  $N_{int}(r)$  random numbers following a Poisson distribution of parameter  $\bar{t}(r)$ , determine the arithmetic mean and compute the contrast. The result is show on Figure 10 which is clearly different from the results observed on data.

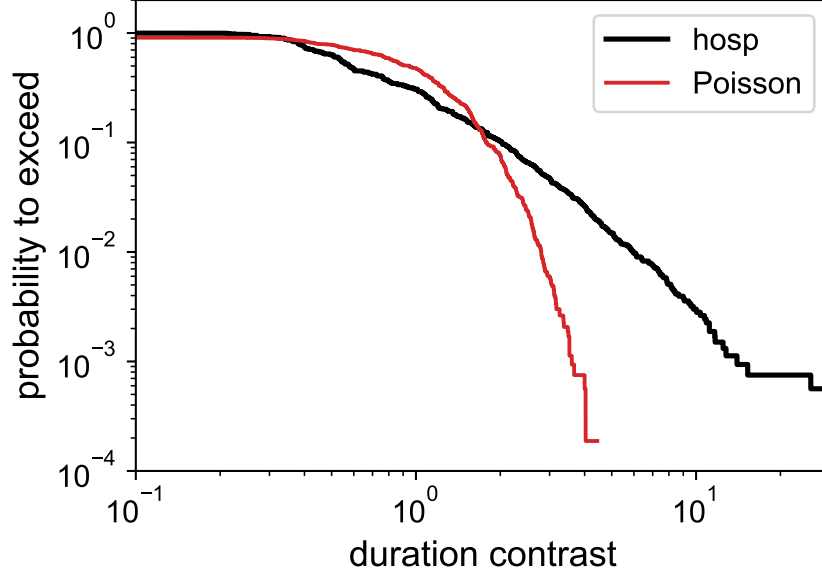


Figure 10: Distribution of the contrast durations assuming Poisson distributed durations. The parameters are taken from the *hosp* dataset and the data result is recalled in red.

## S7 Dimension above 2

A Levy flight can be generalized to any dimension (see [7] for a simple algorithm). For our model, we have tried several dimension. Figure 11 shows the result in dimension 3 (note that the coefficients  $A$  and  $\alpha_c$  from Sect. S5 have been recomputed). Compared to dimension 2 (see Figure 2 (c)), the agreement with the *malawi* data gets worse. If we further increase the dimension the return probability of the walk decreases and the contrast goes to  $\exp(-\delta)$  which is clearly far from the data.



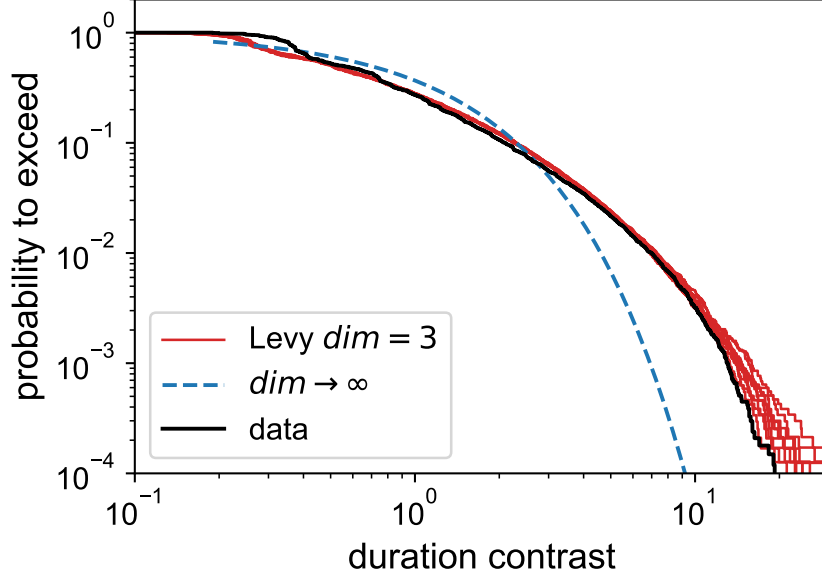


Figure 11: Levy model ( $\alpha = 1.1$ ) in red compared to the *malawi* data (in black) for a Levy walk in a space of dimension 3. Increasing the dimension further, the model converges to the dashed blue line.

## S8 Effect of the time resolution

The timing resolution of the experiments affects our model in two ways. The size and scale of each LGG (thus relation) are given by

$$N(r) = \sum_{i=1}^{N_{int}(r)} t_i(r) \quad (2)$$

$$s(r) = [A\bar{t}(r)]^{1/\alpha_c} \quad (3)$$

where  $A \simeq 1$ ,  $\alpha_c \simeq \alpha$  (see Sect. S5).

$t_i$  and  $\bar{t}$  are expressed as a number of resolution steps (which in the paper is  $T = 20$  s). We may artificially change it, assuming for instance a resolution of  $T = 5$  s, in which case we multiply the  $t_i$ 's and  $\bar{t}$  by a factor 4. This changes for each graph the values of  $N$  and  $s$ . The result on the contrast distribution for this model are shown on Figure 12.

Compared to Figure 2(c) this model fits less well the data which is normal since we have used a fake resolution. It shows that the wiggles at the beginning of the distribution are due to the  $T = 20$  s resolution. A prediction from our model is thus that the contrast distribution should be smoother and slightly different if we have data with a better timing resolution.

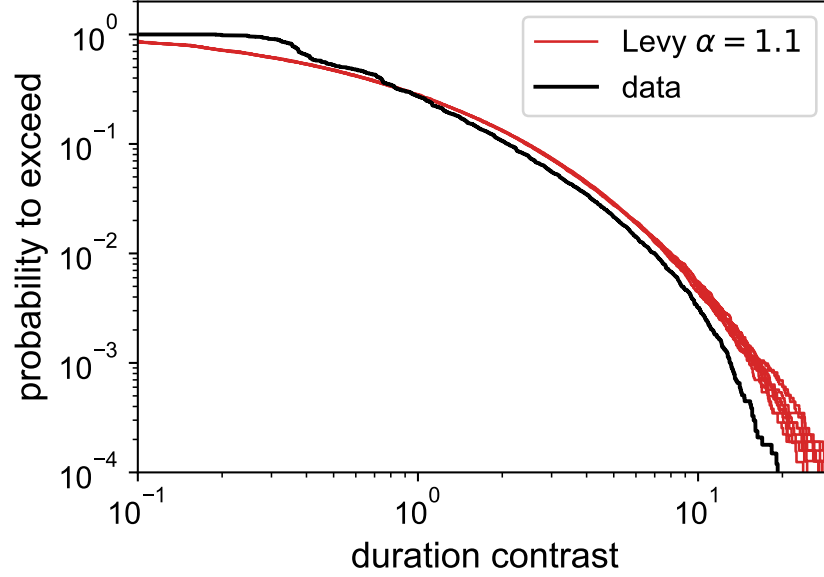


Figure 12: Levy model ( $\alpha = 1.1$ ) modified by increasing the resolution to  $T=5$  s (red curves) compared to the *malawi* dataset.

## References

- [1] Ciro Cattuto, Wouter Van den Broeck, Alain Barrat, Vittoria Colizza, Jean-François Pinton, and Alessandro Vespignani. Dynamics of Person-to-Person Interactions from Distributed RFID Sensor Networks. *PLoS ONE*, 5(7):e11596, July 2010.
- [2] Juliette Stehlé, Nicolas Voirin, Alain Barrat, Ciro Cattuto, Vittoria Colizza, Lorenzo Isella, Corinne Régis, Jean-François Pinton, Nagham Khanafer, Wouter Van den Broeck, and Philippe Vanhems. Simulation of an SEIR infectious disease model on the dynamic contact network of conference attendees. *BMC Medicine*, 9(1):87, December 2011.
- [3] Mathieu Génois, Christian L. Vestergaard, Julie Fournet, André Panisson, Isabelle Bonmarin, and Alain Barrat. Data on face-to-face contacts in an office building suggest a low-cost vaccination strategy based on community linkers. *Network Science*, 3(3):326–347, September 2015.
- [4] Mathieu Génois and Alain Barrat. Can co-location be used as a proxy for face-to-face contacts? *EPJ Data Science*, 7(1):11, May 2018.
- [5] Julie Fournet and Alain Barrat. Contact Patterns among High School Students. *PLoS ONE*, 9(9):e107878, September 2014.
- [6] Rossana Mastrandrea, Julie Fournet, and Alain Barrat. Contact patterns in a high school: A comparison between data collected using wearable sensors, contact diaries and friendship surveys. *PLoS ONE*, 10(9):e0136497, 09 2015.
- [7] S. Plaszczynski, G. Nakamura, C. Deroulers, B. Grammaticos, and M. Badoual. Levy geometric graphs. *Phys. Rev. E*, 105:054151, May 2022.